Corrosion Science 51 (2009) 785–792

Contents lists available at ScienceDirect

Corrosion Science

journal homepage: www.elsevier.com/locate/corsci

Changes in the passive layer of corrugated austenitic stainless steel of low nickel content due to exposure to simulated pore solutions

A. Bautista [a,*], G. Blanco [a], F. Velasco [a], A. Gutiérrez [b], L. Soriano [b], F.J. Palomares [c], H. Takenouti [d]

[a] Departamento de Ciencia e Ingeniería de Materiales e Ingeniería Química, Universidad Carlos III de Madrid, Avda Universidad no. 30, 28911 Leganés, Madrid, Spain
[b] Departamento de Física Aplicada and Instituto de Ciencia de Materiales Nicolás Cabrera, Universidad Autónoma de Madrid, Cantoblanco, 28049 Madrid, Spain
[c] Instituto de Ciencia de Materiales de Madrid (ICMM), Consejo Superior de Investigaciones Científicas (CSIC), Cantoblanco, Madrid, Spain
[d] UPR-15 du CNRS, UPMC, 4 place Jussieu, 75252 París Cedex 05, France

ARTICLE INFO

Article history:
Received 16 September 2008
Accepted 23 January 2009
Available online 31 January 2009

Keywords:
A. Concrete
A. Stainless steel
B. EIS
B. XPS
C. Passive films

ABSTRACT

In this work, changes undergone at the passive layer of a new type of corrugated austenitic stainless steel (low Ni, high Mn 204Cu type) when exposed to solutions simulating that contained in the pores of concrete have been studied. Changes in the nature of the passive layer have been characterized by X-ray photoelectronic spectroscopy (XPS) and electrochemical impedance spectroscopy (EIS). Particular focus has been put on the influence of the presence of chlorides and/or carbonation in the solution. Changes in the passive layer due to the passivation treatment that is often applied to corrugated stainless steels during manufacturing processes have also been considered. The results obtained on the 204Cu type steel have been compared with those obtained on more traditional, high Ni, austenitic AISI 304 grade and duplex SAF 2205 grade. During the immersion in simulated pore solutions, 204Cu type suffers more intense redox processes than other studied stainless steels. Moreover, it shows less Cr-rich protective passive layers in these media.

1. Introduction

The durability of reinforced concrete structures (RCS) is favoured by the formation of a passive layer on the surface of the carbon steel embedded in them due to their alkalinity (pH ≈ 13.6). However, carbon steel in concrete often loses its passivity due to the presence of chlorides in marine environments or from the de-icing salts, or to atmospheric CO_2 that produces carbonation of the concrete and reduces its pH. A wide variety of protection methods has been proposed to prevent the corrosion of RCS structures exposed to aggressive environments, being the most important: cathodic protection [1], chemical inhibitors [2], epoxy coatings on reinforcements [3], reinforcement galvanization [3] and concrete waterproofing [4,5]. All methods mentioned have drawbacks or limitations discussed in the bibliography [3,4,6–8].

Stainless steel reinforcements were first used many decades ago and have proved their ability to avoid corrosion problems for a very long time, even in very aggressive conditions [9]. Hence, the use of stainless-steel reinforcements is one of the most reliable methods for ensuring RCS durability. However, their use has been limited for decades due to the higher cost of stainless steels as compared with carbon steels. In practice, however, for preventing corrosive attacks, stainless-steel reinforcements need to be used only in the most critical areas of the structures (such as tidal zones in bridges in marine regions). Moreover, some studies have shown that stainless-steel reinforcements may be less expensive than other alternatives in the long term, since they involve great saving in maintenance costs [10]. The cost-effectiveness limit of the use of stainless steel at the splash zones has been fixed at 14% higher than the cost of using carbon steel reinforcements [11].

During the last years, the use of stainless steel reinforcements is becoming more frequent. There are interesting studies focused on the corrosion behaviour of traditional corrugated austenitic types – such as AISI 304 or 316 – in concrete [12]. On the other hand, duplex SAF 2205 stainless steel has proved its exceptional corrosion resistance in simulated concrete media [13] and it is manufactured for RCS in extremely aggressive environments. New low Ni, high Mn types [14–16] have also been considered interesting for economical reasons and electrochemical studies carried out with *dc* techniques have shown lower corrosion resistance as compared with traditional austenitic types such as AISI 304; however, these steels could be adequate for RCS in many environments. Further low-term studies in concrete are necessary to reach a deep knowledge of the corrosion behaviour of low-Ni stainless steels in concrete. Moreover, the nature of the passive films formed in these materials and the way in which the solution inside the pores of the concrete modifies them are also very interesting features to know.

* Corresponding author. Fax: +34 91 624 9430.
E-mail address: mbautist@ing.uc3m.es (A. Bautista).

0010-938X/$ - see front matter © 2009 Elsevier Ltd. All rights reserved.
doi:10.1016/j.corsci.2009.01.012

The passive films formed in carbon steel in pore solutions have been identified by XPS as composed of Fe_2O_3 covered by a thin layer of goethite [17]. There are previous studies carried out by other authors on the passivation of AISI 316 stainless steel foil in alkaline media; however, these studies are more focused on the presence of Ca adsorbed from the media than on the nature of passive films [18,19]. On the other hand, Abreu et al. have published several studies about oxide layers electrochemically thickened in NaOH solutions on ferritic, austenitic and duplex stainless steels [20–23].

In this work, changes undergone at the passive layer of the new type 204Cu (low Ni, high Mn austenitic stainless steel) is studied when exposed to solutions that simulate that contained in the pores of the concrete with different levels of contamination (chlorides, carbonation). More traditional, high Ni, austenitic AISI 304 type and duplex SAF 2205 type are also studied in the same conditions for comparison.

2. Experimental procedure

The compositions of the three corrugated stainless-steel bars used for this study are shown in Table 1. All the studied materials were cold formed. Diameters and mechanical properties are shown in Table 2.

The chemical composition of the passive layers formed on stainless steels has been studied by X-ray photoelectronic spectroscopy (XPS). For these studies, corrugated bars were always previously machined to obtain flat surfaces from longitudinal sections, in order to avoid noise in the XPS measurements. Intensive cleaning of samples was carried out with polar and non-polar solvents before immersion. The surfaces of the specimens have been studied in different conditions: the natural passive layer formed spontaneously in air, the protective layer that appears after the passivating treatment often carried out in the industry (immersion in 60% w/w HNO_3 for 2 min), and the passive layer formed after 10 days of immersion in different simulated pore solutions. These were $Ca(OH)_2$ saturated non-carbonated solutions (pH ≈ 12.6), in some cases without chlorides, and in other cases with 1% w/w NaCl. Studies have also been carried out in $Ca(OH)_2$ saturated solutions carbonated by bubbling with CO_2-rich air to pH ≈ 9 (also with and without chlorides). 204Cu stainless steels were also measured after exposures to $Ca(OH)_2$ solutions whose pH has been decreased down to about 7 by using CO_2. Three samples of 204Cu and two samples of 304 and 2205 stainless steels were tested in all conditions.

XPS measurements were carried out in a standard surface analysis chamber equipped with a dual anode (Mg and Al) X-ray source and a VG CLAM4 hemispherical electron analyzer. Some of the measurements were done using a Specs Phoibos 250 electron analyzer under the same experimental conditions. Before placing the samples in the vacuum chamber, they were dried with pressurized nitrogen but no other surface cleaning was used so as not to modify their composition or oxidation state. The sensitivity factors of the elements have been taken into account when calculating relative concentrations in the passive layer studied. Experimental data have been minimum-squares fitted, using Lorentz functions for photoemission peaks and hirley's background. The resulting curve was then convoluted with a Gaussian function to simulate the experimental resolution, which has been found to be 0.67 eV.

Changes in the passive layer due to the immersion in simulated pore solutions have been monitorized by electrochemical impedance spectroscopy (EIS). Two different kinds of samples have been used for these studies. In one case, samples have been extracted from the core of the corrugated bar reinforcements, and then the cross section of this core was exposed to solution. For this, reinforcement diameters have been mechanically reduced to about 4.9 mm. To avoid crevice problems during testing, the resulting cores have been organic coated via cataphoresis before resin embedding. The mounted samples have left a cross-section of the core of the bars as exposed surface. The cross sections have been mechanically polished up to grade 320 with SiC. The second type of samples has consisted of pieces of corrugated bars that had previously suffered a passivating treatment in HNO_3 during their industrial manufacturing process. The corrugated surface of these samples has not been modified in any way for lab measurements, while the cross section immersed in the simulated pore solution has been polished up to grade 320 with SiC. Two centimeter length sections of corrugated bars have been immersed in simulated pore solutions.

The cross-sections of the cores were monitorized by EIS during the first 32 h of immersion in the solutions. EIS measurements were started 10 s after specimens had been exposed. During the first nine measurements, the frequency scanning range was varied from 10 kHz to 10 mHz and the interval between the end of a measurement and the beginning of the next one was 60 s. From the tenth measurement on, spectra have been registered between 10 kHz and 2 mHz at 1-h intervals. The final spectra have been obtained over an interval between 10 kHz and 1 mHz, and the time between measurements was increased to 2 h. For these measurements two different solutions have been considered: non-carbonated saturated $Ca(OH)_2$ solutions without chlorides and with 0.5% of NaCl.

EIS measurements performed on the surface of the corrugated bars have been carried out after 2 and 18 h of exposure to the solutions, with a frequency scan ranging from 100 kHz to 1 mHz. For these measurements six different solutions were considered: non-carbonated and carbonated saturated $Ca(OH)_2$ solutions with 0%, 0.5% and 5% of NaCl.

Impedance measurements were carried out using a saturated calomel electrode (SCE) as reference, and a platinum mesh as counter-electrode. All the impedance spectra obtained were fitted and simulated with a SIMPLEX-based software.

Table 2
Diameter and tensile test results of the studied stainless steels.

AISI type	Nominal diameter (mm)	Actual outer diameter (mm)	TS (MPa)	σ_y (MPa)
204Cu	5	5.2–5.4	918	756
304	10	10.0–10.5	968	812
2205	10	10.2–10.4	1170	960

Table 1
Chemical composition of the studied corrugated stainless steels.

Type	%Cr	%Ni	%Mo	%Mn	%S	%C	%Si	%Cu	%N	%Fe
204Cu	16.5	1.93	0.07	7.94	0.001	0.060	0.28	2.69	0.13	*Bal.*
304	18.45	8.34	0.21	1.41	0.004	0.056	0.30	0.20	0.06	*Bal.*
2205	22.12	4.47	3.22	1.62	0.001	0.025	0.33	0.10	0.18	*Bal.*

The corrosion potential of both type of samples used in electrochemical measurements in solutions in sealed recipients (to avoid carbonation).was monitorized vs SCE for 30 days.

3. Results

XPS results show that the passive layer on 204Cu stainless steels is mainly formed by Fe and Cr oxides. However, as it can be seen in Fig. 1, oxidized Cu and Mn have also been detected in variable amounts depending on exposure conditions. The Cu content of the passive layer tends to increase when chlorides are present in the simulated pore solution. The nitric passivated surface exhibits a passive layer with a higher proportion of protective Cr_2O_3. Samples exposed to non-carbonated solutions (pH ≅ 13) have Cr_2O_3 content in the passive layer intermediate between those of passivated samples and those of the samples with untreated surface (i.e., only air exposed). The passive layer on samples exposed to carbonated solutions (pH ≅ 9) shows the lowest proportion of Cr_2O_3 in their passive layer. The presence of chlorides in the solution does not affect the chromium content in the passive layer.

Fig. 2 shows the ratio between Cr^{3+} concentration and the rest of metallic cations detected by XPS at the passive layers of 204Cu, 304 and 2205 stainless steels for the different exposure conditions studied. Apart from Cr, oxidized Fe, Cu and Mn were detected for 204Cu (Fig. 1); only oxidized Fe was found in 304, and oxidized Fe and Mo (the latter only at pH 9 and in small amounts) were found in 2205 grade. XPS measurements on duplex 2205 and austenitic 304 specimens have shown only the presence of Fe and Cr as oxidized metallic cations in the passive layer. The tendencies observed in Fig. 1 concerning the influence of the medium on the content of Cr_2O_3 in the passive layer for 204Cu stainless steel are confirmed in Fig. 2 for 2205 and 304 stainless steels: (a) Both the nitric acid passivating treatment and the exposure to non-carbonated solutions increase Cr^{3+} concentration in comparison with that in the passive layer formed in air; (b) Exposition to carbonated solutions decreases Cr_2O_3 content; and (c) The presence of chlorides in the environment does not affect Cr_2O_3 concentration in the passive layer. It also becomes clear from Fig. 2 that the 2205 type always shows the highest Cr_2O_3 content in the passive layer of all the three studied stainless steels studied, while the 204Cu type shows the lowest. The differences in Cr_2O_3 content observed in air between 204Cu type and traditional, high-Ni 304 type tend to increase after exposure to HNO_3 or simulated pore solutions.

The ratio between metallic cations and non-oxidized metallic atoms detected in the XPS spectra is shown in Fig. 3 for 204Cu type specimens. This ratio can be used as an approximate indicator of the relative thickness of passive films. As it can be seen in Fig. 3, the thinnest passive layer is obtained for the nitric passivated condition. The thickness of the layer after immersion in simulated pore solutions is very pH-dependent: the non-oxidized metal signal in the spectra decreases as the alkalinity of the medium does. The presence of chlorides in the simulated pore solution does not affect the thickness of the passive layers. The passive layer formed in air has a thickness between those of the layers formed in non-carbonated solutions and those of the layers formed in solutions carbonated up to pH 9. A further decrease of the pH down to 7 promotes an increase on the thickness of the passive layer.

In Fig. 3, it can also be observed that the trend for the ratio metallic cations/metals in the 304 steel due to the influence of the media is similar to that observed for the 204Cu stainless steel. For the 304 type, and especially for the duplex stainless steel, this ratio suffers more moderate changes with the exposure conditions tested than it does for austenitic stainless steels.

Fe cations in the passive layer of 204Cu stainless steels are present both as Fe^{2+} and Fe^{3+}, as determined by XPS. Fig. 4 shows as an example the deconvolution of the XPS Fe peak of 204Cu steel in a non-carbonated pore solution without chlorides, with the presence of both cationic species. Fig. 5 shows the Fe^{2+}/Fe^{3+} ratio found in the passive layers of the three stainless steels studied in different conditions. As it can be seen, the Fe^{2+} content is higher for the three materials – and more markedly for the duplex stainless steel – after the passivation treatment. Exposure to alkaline solutions also tends to increase the relative amount of Fe^{2+} as compared to that observed in the passive layer formed in air. Fig. 6 shows the influence of pH and chloride content of the solution on the Fe^{2+}/Fe^{3+} ratio obtained for 204Cu stainless steel. Fe^{2+} relative amount decreases as the pH of the $Ca(OH)_2$ solution does. The presence of chlorides in the solution does not have a meaningful influence on this parameter.

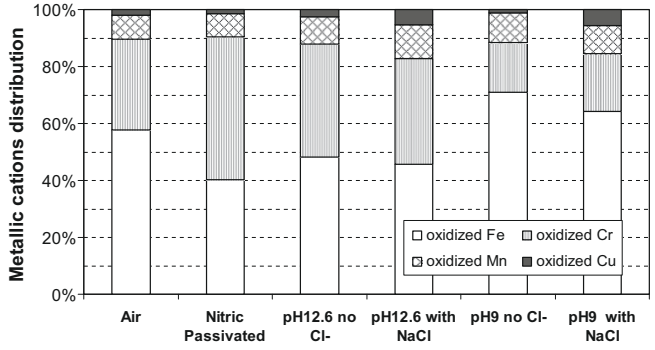

Fig. 1. Metallic cations of the oxides that form the passive layer on 204Cu stainless steel in different conditions as obtained from quantitative XPS analysis.

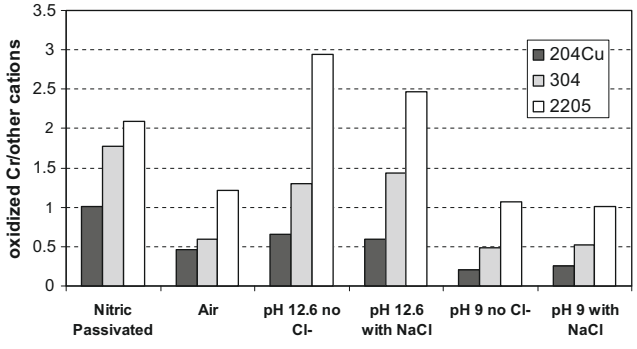

Fig. 2. Ratio between the concentrations of oxidized Cr and other oxidized metallic cations in the passive layer formed in the three studied stainless steels in different conditions as obtained from quantitative XPS analysis.

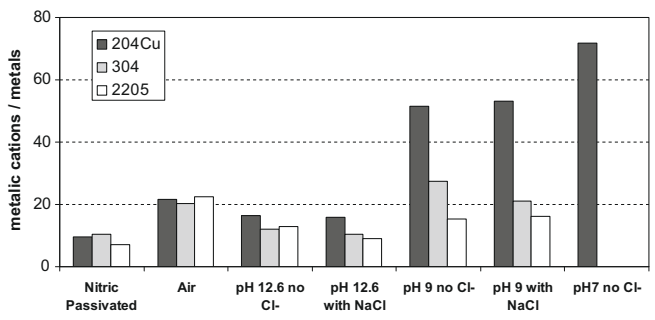

Fig. 3. Metallic cations/metal ratio as observed in the XPS spectra for 204Cu stainless steel in different conditions.

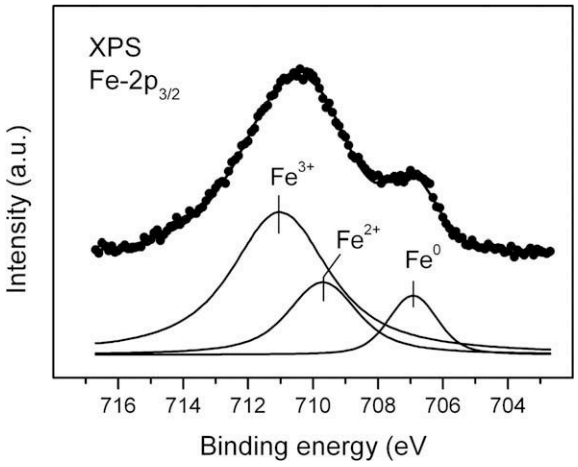

Fig. 4. Deconvolution of the Fe 2p 3/2 XPS spectrum of the 204Cu stainless steel in non-carbonated, saturated $Ca(OH)_2$ solution without chlorides.

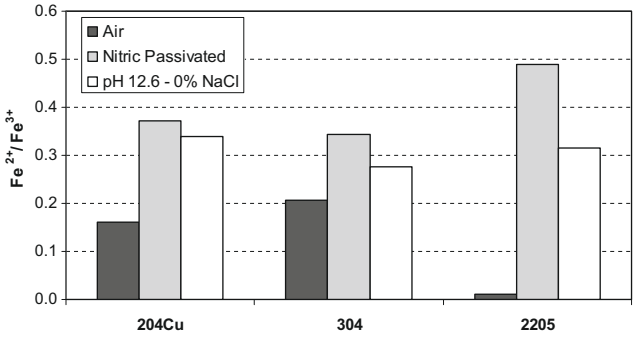

Fig. 5. Fe^{2+}/Fe^{3+} ratio as observed by XPS for the passive layer on the three studied stainless steels, formed in air, in nitric acid and in non-carbonated, $Ca(OH)_2$ solution.

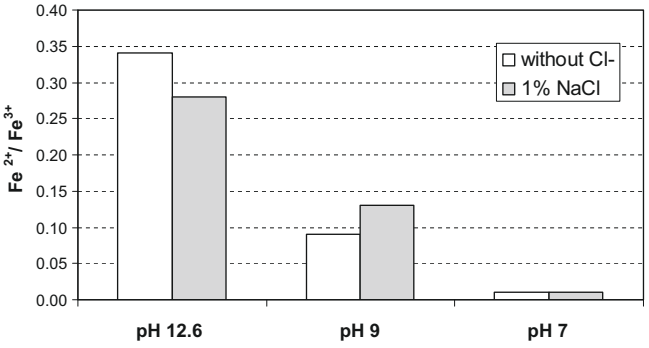

Fig. 6. Fe^{2+}/Fe^{3+} ratio as observed by XPS by XPS for the passive layer on 204Cu stainless steels formed in $Ca(OH)_2$ solutions with different pHs and chloride levels.

Additionally to the XPS measurements, EIS measurements were also carried out on the different species. Fig. 7 shows as an example a typical EIS spectrum obtained on 204Cu steel after immersion in non-carbonated, saturated $Ca(OH)_2$ solution with 1% NaCl. An analysis of the experimental data with standard simulation methods revealed that all spectra show two time constants quite overlapped. The model selected to interpret was the two-time-constant cascade, which seems to be able to afford the most coherent physical interpretation of the results. This equivalent circuit also provides a very good fit of experimental data, as it can also be seen in Fig. 7.

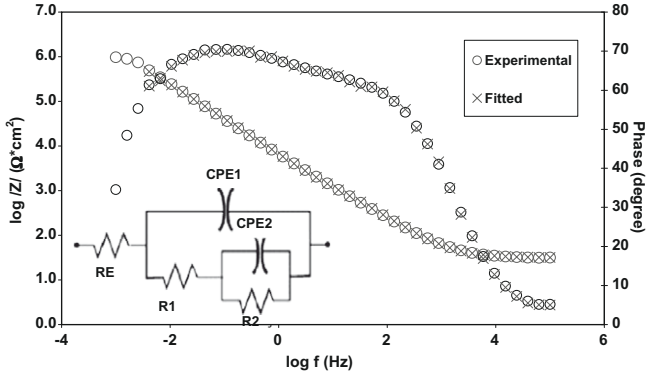

Fig. 7. EIS spectrum corresponding to 204Cu after 20 h in a non-carbonated, saturated $Ca(OH)_2$ solution with 1% NaCl (experimental and simulated data).

The values of the most interesting parameters obtained by simulation of the EIS spectra can be seen in the example shown in Fig. 8, which corresponds to 204Cu after 2 h of exposure in $Ca(OH)_2$ saturated solution without chlorides. These values are the capacity corresponding to the constant phase element of the medium frequency time constant, *C*1, the capacity corresponding to the constant phase element of the low frequency time constant, *C*2, the resistance corresponding to the medium frequency time constant, *R*1, and the resistance corresponding to the lower frequency time constant, *R*2. The influence of the presence of a corrugated surface can also be seen in this figure. The exact value of some parameters can be uncertain due to the overlapping of the two time constants detected in the spectra. However, after analyzing a considerable amount of spectra, the following tendencies have been found. In general, for ribbed samples, *C*1 and *C*2 have a value close to 10^{-5} F cm^{-2}. For samples extracted from the core of the bars, the *C*1 values hardly change, while *C*2 tends to be somewhat higher. For ribbed samples, *R*1 shows values in the kΩ range, while much higher values are found for *R*2. Both *R*1 and *R*2 show lower values for spectra from samples extracted from the core of the bars.

*C*1 and *C*2 hardly change their values after exposure to the simulated pore solution, but, on the other hand, *R*1 and *R*2 tend to increase. As it can be observed in Fig. 9, increases of about one order of magnitude have been detected in these parameters during the tests carried out.

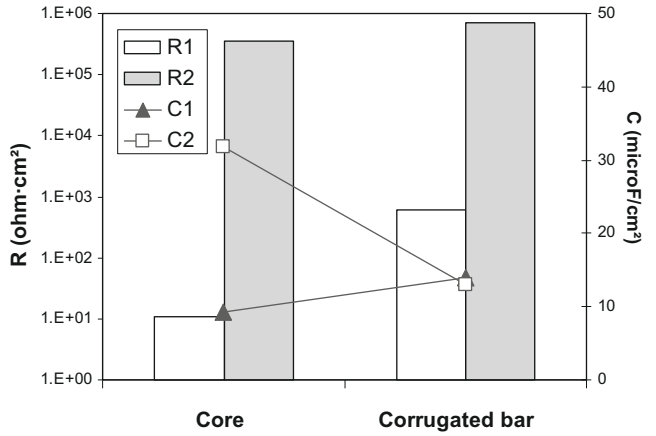

Fig. 8. Differences between the values for the EIS parameters obtained from the impedance spectra when the electrochemical measurements are performed on the core of the bar or on the as-received surface of 204Cu reinforcements exposed for 2 h in non-carbonated, saturated $Ca(OH)_2$ solutions without NaCl.

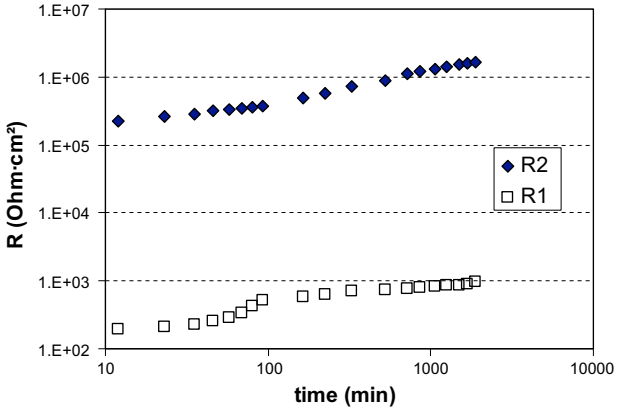

Fig. 9. Increase with the immersion time of the *R*1 and *R*2 values obtained from the EIS spectra of 204Cu samples in non-carbonated $Ca(OH)_2$ solutions with 0.5% NaCl.

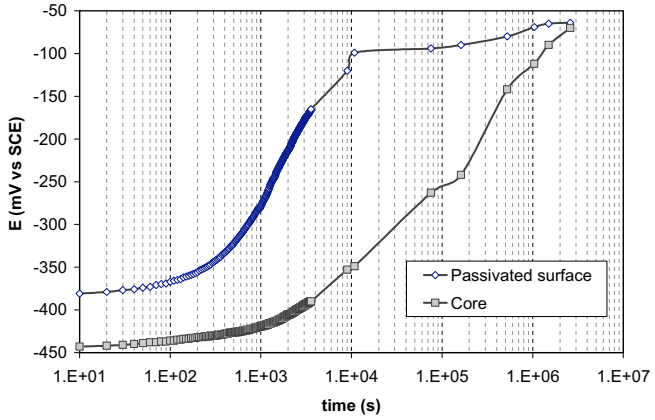

Fig. 10. Differences between the E_{corr} when the electrochemical measurements are performed on the core of the bar or on the as-received surface of the reinforcement. The data correspond to 204Cu stainless steel after 2 h of exposure in non-carbonated solutions.

Another important difference found between ribbed samples and core samples is the lower corrosion potential (E_{corr}) measured on the non-ribbed samples at the beginning of the exposure to saturated $Ca(OH)_2$ solutions with chlorides (Fig. 10). As the exposure goes on, E_{corr} increases for both types of samples and tends to become closer.

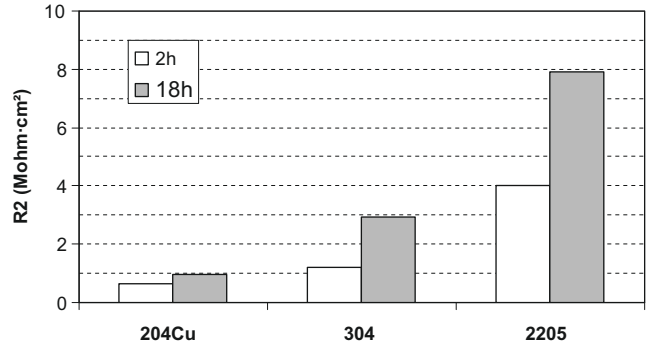

Fig. 11. Influence of the chemical composition of the reinforcement on the *R*2 value obtained from EIS spectra of corrugated bars exposed in non-carbonated, saturated $Ca(OH)_2$ solutions with 0.5 NaCl. The effect of the exposure time is also shown.

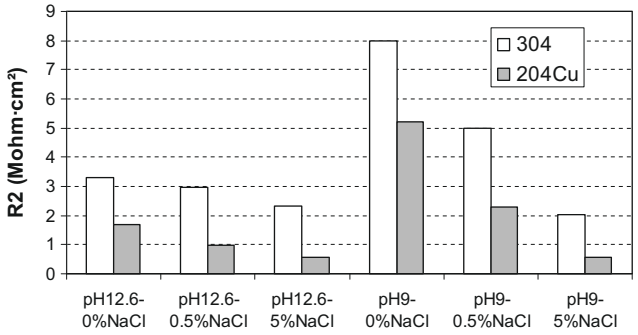

Fig. 12. Influence of the pH and chloride content on the *R*2 values obtained form EIS measurements of as-received surfaces of the austenitic reinforcements.

*R*2 values are conditioned by stainless-steels' composition. For a given solution and a given exposure time, *R*2 values are higher for 2205 and lower for 204Cu, while they reach intermediate values for 304 (Fig. 11). This figure confirms one of the trends shown in Fig. 9: *R*2 always tends to increase along with exposure time in the simulated pore solution independently of the composition of the solution or the type of sample used.

*R*2 also depends on the pH of the media where stainless-steel samples are immersed: it tends to be higher in carbonated media than in non-carbonated media (Fig. 12). Moreover, the chloride content tends to decrease *R*2, being the effect of chlorides more marked in carbonated solutions than in non-carbonated ones.

4. Discussion

XPS results proved that the exposure of stainless steels to simulated pore solutions modifies the composition of their passive layers. On pH 12.6 media, the passive film on stainless steels becomes chromium richer, as compared with those formed on air (Figs. 1 and 2). The higher presence of Cr_2O_3 makes the film thinner (Fig. 3). Neither Ni-enrichment (which has been detected by other authors for AISI 316 type [19]) nor any other meaningful change in the composition of the passive layers on 304 and 2205 have been detected due to the addition of chlorides to the saturated $Ca(OH)_2$ solution. These results explain the good behaviour that traditional stainless-steel rebars have shown in concrete structures exposed to aggressive marine environments [9].

The differences detected in the passive layers due to the chemical composition of the base metal can also explain the differences in the corrosion behaviour of stainless steels detected by *dc* tests at the same pHs (12.6 and 9) and chloride concentrations from 0% to 5% [13,14]. The impossibility of causing pitting by polarization curves of the duplex stainless steels – in spite of the high chloride concentration in the solution – is coherent with the high chromium content in their passive layer (Fig. 2). The stability of the passivity for austenitic 304 – which only pits at high overpotentials in presence of chlorides – is also coherent with the Cr_2O_3 presence in its passive layer in $Ca(OH)_2$ solutions: the quantity of Cr_2O_3 is lower than that in 2205, but around double of that detected for the passive layer on 304 in air (Fig. 2). The chemical composition of the passive layer also explains the behaviour of 204Cu, whose results in non-carbonated $Ca(OH)_2$ solutions have suggested that it could be an interesting alternative for non-carbonated concrete with a moderate chloride content [14]. Alkaline pH favours Cr enrichment of the passive layer on 204Cu (Fig. 1). This Cr-enrichment of the passive layer in non-carbonated solutions (when they are compared with the air-formed ones) has also been detected for 304 and 2205 stainless steels to greater extent (Fig. 2). Moreover, the presence of Mn and Cu in 204Cu stainless steel (Table 1) also

promotes thicker passive layers (Fig. 3), since these elements are easily oxidized. On the other hand, chlorides in the media favour higher presence of Cu oxides in the passive layer of 204Cu types (Fig. 1). The presence of this element has proved to be very effective to improve corrosion behaviour of stainless steels in media with low pH [24]. Cu additions to stainless steels are probably also useful in alkaline media due to the sensibility of the copper to the chlorides, but further tests should be carried out to confirm this point.

Exposure of stainless steels to a medium that simulates carbonated concrete makes the passive films to thicken (Fig. 3) and the chromium content of the passive layer to be reduced (Fig. 2) if they are compared with the air-formed passive layers. The intensity of these changes depends a lot on the composition of the base steel. The passive layer of 2205 exhibits high Cr-content (Fig. 2), which is coherent with the absence of corrosion after potentiodinamic tests in this medium [25]. The chemical composition of the passive layer of austenitic types seems to be more sensitive to a decrease of the pH of the media, showing a decrease of the Cr content (Figs. 1 and 2). Consequently, passive layers become thicker (Fig. 3) and more prone to generalized corrosion when they are anodically polarized [14]. The corrosion performance of 204Cu is closer to that of 304 in non-carbonated media with chlorides than in carbonated media with chlorides [15]. This can be related to difference on the thickness of the passive layer of both austenitic stainless steels, which is much higher at pH 9 than at pH 12.6 (Fig. 3), suggesting a higher difference between their protective abilities in carbonated media. The differences detected for 204Cu and 304 in the ratio of oxidized Cr and other cations in pH 12.6 and 9 (Fig. 2) are not so marked (204Cu passive layers tend to exhibit ratio twice those of 304), so it is not the Fe/Cr content, but the Mn presence in the passive layer of 204Cu (Fig. 1) the factor determining the differences on passive layer thickness of both austenitic stainless steels and their corrosion behaviour in carbonated media with chlorides. The decrease on the pH of the solution increases the negative effect of Mn oxides on the protective abilities of the passive layers.

In general, the chemical characterization of passive films spontaneously formed on stainless steels in alkaline media has proved that these layers are chromium richer (Fig. 2); that is, much more protective than the electrochemically thicken ones that have been exhaustively characterized by other authors [20–23].

XPS analysis of the different iron oxides present in the passive layer shows that both Fe^{3+} and Fe^{2+} can be found in different proportions (Fig. 4). According to literature, alkaline pHs favour the formation of magnetite on carbon steels [26–28], while on air, Fe^{3+} oxides such as γ-FeOOH are the main components [26–28]. Fe oxides found on stainless steels in air are also much richer in Fe^{3+} than in Fe^{2+} (Fig. 5), as it occurs with carbon steels. The Fe^{2+}/Fe^{3+} content of the passive layer on stainless steels increases when exposed to alkaline solutions (Fig. 5), suggesting that part of the Fe oxide has been transformed into magnetite, as the layer has also become thinner (Fig. 3). Exposure to carbonated solutions favours the formation of Fe^{3+}, as the thickness increased (Fig. 3) – implying an increase of the oxidized Fe content – and the Fe^{2+}/Fe^{3+} ratio tends to decrease (Fig. 6).

On the other hand, the passivating treatment always improves dramatically the protective abilities of the passive layers as compared with those formed on air (Figs. 1–3). Differences between the corrosion resistance of the surface of the reinforcements and the core of the bar have already been detected by other authors [15], though not only the chemical composition of the surface, but also the high concentration of mechanical stresses in the corrugations can affect corrosion resistance [14]. As stainless-steel reinforcements sometimes suffer passivating treatment as a final step in their processing procedure, it would be very interesting to check how the exposure to simulated pore solutions affects their composition, in order to know to what extent the present results can be extrapolated to corrugated stainless steels when they have a previously nitric-passivated surface. The passivating treatment also favours Fe^{2+}-to-Fe^{3+} oxidation to a larger extent than the exposure to non-carbonated solution (Fig. 5).

The clear increase in E_{corr} values in stainless steels due to exposure to simulated pore solutions (Fig. 10) could suggest a change in the cathodic reaction of the system [28]. Lower values of E_{corr} would be associated with the reduction of Fe^{3+} oxides to magnetite, as it has been observed in Fig. 5, when non-passivated surfaces are exposed to basic solutions. The more noble potentials reached after longer immersion time (Fig. 10) suggest that the cathodic reaction would then be an oxygen reduction. The ribbed bars (which have only a part of their surface without being passivated) show higher initial E_{corr} values and a faster subsequent increase due to their immersion in $Ca(OH)_2$ solutions. Since a part of their surface has already been passivated, less Fe^{3+} must be oxidized to magnetite.

The XPS data can also help us understand the physical meaning of the components of the equivalent circuit used for simulation. EIS spectra are the result of the electrochemical reactions that occur at the surface of stainless steel during immersion in simulated pore solutions. These reactions can be metal oxidation (Fe, but also Cr and sometimes Cu and Mn) and redox transformations of the oxides that already formed the passive layer. XPS results show that immersion in simulated pore solution implies Fe^{2+}/Fe^{3+} transformations (Figs. 5 and 6), that means, maghemite–magnetite through the following reaction:

$$4\ Fe_2O_3 + Fe^{2+} + 2e^- \leftrightarrow 3\ Fe_3O_4 \quad (1)$$

This type of maghemite–magnetite transformations has been structurally characterized by other authors [29] and has been considered as the most intense transformation of the oxides in the passive layer that occurs in carbon steels [28,30], as well as in stainless steels in alkaline media [20–23].

Due to the large difference in order of magnitude between both resistances $R1$ and $R2$ (Figs. 8 and 9), the very slow corrosion process that occurs in passive stainless steels (oxidation of the different elements that form the base metal) should be identified with the low frequency time constant. $C2$ has typical values of double layer capacitances for the core material. The lower values observed for $C2$ in the case of the corrugated bars can be understood bearing in mind that not all their surface suffers the intense transformation detected by XPS for the air exposed samples when they are in contact with alkaline media, because part of it has been already passivated.

Analysing the physical meaning of the medium-frequencies time constant, no relationship has been found between the evolution of $R1$ and $C1$, and the changes in the dielectric characteristics of the passive films due to the exposure of stainless steels to the simulated pore solutions were associated with the changes in thickness and composition detected by XPS (Figs. 2 and 3). Hence, it cannot be identified with the passive layer. On the other hand, for carbon steels reinforcements, the time constant that appears at medium frequencies in the impedance spectra has been sometimes associated in the bibliography with to the presence of hydroxides adsorbed on the surface of the reinforcements [31,32]. This is a plausible interpretation that can be also applied to stainless steel reinforcements in $Ca(OH)_2$ solutions. It is logical that resistance of precipitated hydroxide layers tend to increase during the onset of the exposure to simulated pore solutions (Fig. 9). However, another option could be to identify it with the transformations of the Fe oxides that form the most external region of the passive layer (Eq. (1)). The influence of this reaction in the EIS spectra has also been suggested previously in the bibliography

[13,20–23]. In this case, the increase of $R1$ with exposure time (Fig. 9) should correspond to the lower rate of the transformations of Fe oxides, since their oxidation state is more similar to that favoured by the pH of the solution at the equilibrium (Figs. 5 and 6).

The high $R2$ values shown by the duplex stainless steels and the low ones of the low-Ni stainless steels seem to be related to different protective abilities of the films formed on the stainless steels studied (Fig. 11). Moreover, a small decrease of $R2$ can be also detected when chlorides are added to simulated pore solutions (Fig. 12). The small effect of the chlorides observed in our study is coherent with the corrosion rates obtained by other authors for high-Ni austenitic stainless steels by using polarization resistance measurements [33].

The trend of $R2$ to increase when stainless steels reinforcements are exposed to carbonated pore solutions instead of non-carbonated pore solutions is more difficult to explain (Fig. 12). The effect of the pH on $R2$ has also been observed for corrosion rates of passive stainless steel measured with *dc* techniques [14]. This fact suggests that other factors, besides simple iron oxidation, are affecting $R2$ value. Other phenomena, such as Cr oxidation (that must occur to a larger extent when stainless steels are exposed to non-carbonated media than when they are exposed to carbonated ones) can also appear in this region of the spectra very overlapped with Fe oxidation. The Cr oxidation process that must take place to make the passive layer formed in air reach the composition detected in the simulated pore solution (Figs. 1 and 2) can also influence the impedance at low frequencies. This fact would explain the trend of $R2$ to increase its value as immersion in simulated pore solutions extends (Figs. 9 and 11).

5. Conclusions

1. The chromium content of passive layers formed in simulated pore solutions is higher than those formed in air when the solution is non-carbonated, but lower when the solution is carbonated.
2. The chloride content of the pore simulated solutions does not have a meaningful influence on the composition of the passive layers formed in stainless steels, but promotes small changes in corrosion rates that can be detected by EIS.
3. The intensity of the electrochemical changes occurring on the corrugated surface and the core of the stainless-steel reinforcements when they are exposed to simulated pore solutions is different.
4. 204Cu types show lower Cr-content in the passive layer than other studied stainless steels in simulated pore solutions. Moreover, they exhibit a meaningful presence of poorly-protective Mn oxides.
5. The electrochemical transformations detected by EIS when 204Cu stainless steels are exposed to simulated pore solutions are more intense than those shown for other stainless steels, confirmating the poorer quality of their passivity.

Acknowledgements

The authors thank the firm Roldán S.A. (ACERINOX group) of Spain for providing the corrugated stainless steels used in this study, and the Spanish Ministry of Science and Technology for the financial support provided through the projects MAT2004-06435-C02-02 and MAT2007-66719-C03-03.

References

[1] P. Pedeferri, Cathodic protection and cathodic prevention, Const. Building Mater. 10 (1996) 391–402.
[2] V.T. Ngala, C.L. Page, M.M. Page, Corrosion inhibitor systems for remedial treatment of reinforced concrete. Part 2: sodium monofluorophosphate, Corros. Sci. 45 (2003) 1523–1537.
[3] A.B. Darwin, J.D. Scantlebury, Retarding of corrosion processes on reinforcement bar in concrete with an FBE coating, Cement Concrete Comp. 24 (2002) 73–78.
[4] J.A. González, E. Ramírez, A. Bautista, S. Feliu, The behaviour of pre-rusted steel in concrete, Cement Concrete Res. 26 (1996) 501–511.
[5] M.M. Al-Zahrani, S.U. Al-Dulaijan, M. Ibrahim, H. Saricimen, F.M. Sharif, Effect of waterproofing coatings on steel reinforcement corrosion and physical properties of concrete, Cement Concrete Comp. 24 (2002) 127–137.
[6] L.K. Spainhour, I.A. Wootton, Corrosion process and abatement in reinforced concrete wrapped by fiber reinforced polymer, Cement Concrete Comp. 30 (2008) 535–543.
[7] J.J. Chang, A study of bond degradation of rebar due to cathodic protection current, Cement Concrete Res 32 (2002) 657–663.
[8] J.A. González, E. Ramírez, A. Bautista, Protection of steel embedded in chloride-containing concrete by means of inhibitors, Cement Concrete Res. 28 (1998) 577–589.
[9] P. Castro-Borges, O.T. de Rincón, E.I. Moreno, A.A. Torres-Acosta, M. Martínez-Madrid, A. Knudsen, Performance of a 60-year-old concrete pier with stainless steel reinforcement, Mater. Performance 41 (2002) 50–55.
[10] O. Klinghoffer, T. Frolung, B. Kofoed, A. Knudsen, F.M. Jensen, T. Skovsgaard, Practical and economical aspects of application of austenitic stainless steel, AISI 316, as reinforcement in concrete, in: J. Mietz, R. Polder, B. Elserner (Eds.), Corrosion of Reinforcement in Concrete, European Federation of Corrosion, IOM Communications, London, 2000, pp. 121–133.
[11] D.V. Val, M.G. Stewart, Life-cost analysis of reinforced concrete structures in marine environments, Struct. Saf. 25 (2003) 343–362.
[12] L. Bertolini, P. Pedeferri, Laboratory and field experience on the use of stainless steel to improve durability of reinforced concrete, Corros. Rev. 20 (2002) 129–152.
[13] A. Bautista, G. Blanco, F. Velasco, A. Gutiérrez, S. Palacín, L. Soriano, H. Takenouti, Passivation of duplex stainless steels in solutions simulating chloride-contaminated concrete, Mater. Construcc. 57 (2007) 17–32.
[14] A. Bautista, G. Blanco, F. Velasco, Corrosion behaviour of low-nickel austenitic stainless steel reinforcements: a comparative study in simulated pore solutions, Cement Concrete Res. 36 (2006) 1922–1930.
[15] M.C. García-Alonso, M.L. Escudero, J.M. Miranda, M.I. Vega, F. Capilla, M.J. Correia, M. Salta, A. Bennani, J.A. González, Corrosion behaviour of new stainless steel reinforcing bar embedded in concrete, Cement Concrete Res. 37 (2007) 1463–1471.
[16] M.C. García-Alonso, J.A. González, J.M. Miranda, M.L. Escudero, M.J. Correia, M. Salta, A. Bennani, Corrosion behaviour of innovative stainless steels in mortar, Cement Concrete Res. 37 (2007) 1562–1569.
[17] A. Carnot, I. Frateur, A. Zanna, B. Tribollet, I. Dubouis-Brugger, P. Marcus, Corrosion mechanisms of steel concrete moulds in contact with a demoulding agent studied by EIS and XPS, Corros. Sci. 45 (2003) 2513–2524.
[18] L. Veleva, A.A. Alpuche-Avilés, M.K. Graves-Brook, D.O. Wipf, Electrochemical study and surface analysis of passive films on AISI 316 stainless steel grown in alkaline solutions, J. Electroanalytic Chem. 537 (2002) 85–93.
[19] L. Veleva, A.A. Alpuche-Avilés, M.K. Graves-Brook, D.O. Wipf, Comparative cyclic voltammetry and surface analysis of passive films grown on stainless steel 316 in concrete pore model solutions, J. Electroanalytic. Chem. 538 (2005) 45–53.
[20] C.M. Abreu, M.J. Cristóbal, R. Losada, X.R. Nóvoa, G. Pena, M.C. Pérez, High frequency impedance spectroscopy study of passive films formed on 316 stainless steel in alkaline medium, J. Electroanal. Chem. 572 (2004) 335–345.
[21] C.M. Abreu, M.J. Cristóbal, R. Losada, X.R. Nóvoa, G. Pena, M.C. Pérez, Comparative study of passive films of different stainless steels developed on alkaline medium, Electrochim. Acta 572 (2004) 3049–3056.
[22] C.M. Abreu, M.J. Cristóbal, R. Losada, X.R. Nóvoa, G. Pena, M.C. Pérez, Long-term behaviour of AISI 304L passive layer in chloride containing medium, Electrochim. Acta 51 (2006) 1881–1890.
[23] C.M. Abreu, M.J. Cristóbal, R. Losada, X.R. Nóvoa, G. Pena, M.C. Pérez, The effect of Ni in the electrochemical properties of oxide layers grown on stainless steels, Electrochim. Acta 51 (2006) 2991–3000.
[24] A. Pardo, M.C. Merino, M. Carboneras, F. Viejo, R. Arrabal, J. Muñoz, Influence of Cu and Sn content in the corrosion of AISI 304 and 316 stainless steels in H_2SO_4, Corros. Sci. 48 (2006) 1075–1092.
[25] A. Bautista, G. Blanco, F. Velasco, Resistencia a la corrosión en disoluciones de $Ca(OH)_2$ con cloruros de armaduras de aceros inoxidables austeníticos y duplex, VIII Congreso Nacional de Materiales. Actas del VIII Congreso Nacional de Materiales, Valencia, Spain, 2004, pp. 989–996, ISBN: 84-9705-594-2.
[26] M. Stratmann, K. Bohnnkamp, H.J. Engell, An electrochemical study of phase-transitions in rust layers, Corros. Sci. 23 (1983) 969–985.
[27] H. Antony, L. Legrand, L. Maechal, S. Perrin, Ph. Dillmann, Study of lepidocrocite γ-FeOOH electrochemical reduction in neutral and slightly alkaline solutions at 25 °C, Electrochim. Acta 51 (2005) 745–753.
[28] J.A. González, J.M. Miranda, E. Otero, S. Feliu, Effect of electrochemcially reactive rust layers on the corrosion of steel in a $Ca(OH)_2$ solution, Corros. Sci. 49 (2007) 436–448.

[29] J.P. Jolivet, E. Tronc, Interfacial electron transfer in colloidal spinel iron oxide. Conversion of Fe_3O_4-γFe_2O_3 in aqueous medium, J. Collod. Interf. Sci. 125 (1988) 688–701.
[30] C. Andrade, P. Merino, X.R. Nóvoa, G. Pena, M.C. Pérez, Passivation of reinforcing steel in concrete, Mater. Sci. Forum 192–194 (1995) 891–898.
[31] W. Morris, A. Vico, M. Vázquez, The performance of a migrating corrosion inhibitor suitable for reinforced concrete, J. Appl. Electrochem. 33 (2003) 1183–1189.
[32] Gadadhar Sahoo, R. Balasubramaniam, On the corrosion behaviour of phosphoric irons in simulated concrete solution, Corros. Sci. 50 (2008) 131–143.
[33] M.L. Escudero, M.C. García-Alonso, F. Capilla, J.A. González, Study of the corrosion resistance of stainless steel in solution simulating concrete, 15th International Corrosion Conference, Paper no. 441, Granada, Spain, 2002.